



Cite this: *Phys. Chem. Chem. Phys.*,  
2015, 17, 20574

# Cold water cleaning of brain proteins, biofilm and bone – harnessing an ultrasonically activated stream†

P. R. Birkin,<sup>\*a</sup> D. G. Offin,<sup>a</sup> C. J. B. Vian,<sup>a</sup> R. P. Howlin,<sup>b</sup> J. I. Dawson,<sup>c</sup> T. J. Secker,<sup>d</sup>  
R. C. Hervé,<sup>d</sup> P. Stoodley,<sup>b</sup> R. O. C. Oreffo,<sup>c</sup> C. W. Keevil<sup>d</sup> and T. G. Leighton<sup>e</sup>

In the absence of sufficient cleaning of medical instruments, contamination and infection can result in serious consequences for the health sector and remains a significant unmet challenge. In this paper we describe a novel cleaning system reliant on cavitation action created in a free flowing fluid stream where ultrasonic transmission to a surface, through the stream, is achieved using careful design and control of the device architecture, sound field and the materials employed. Cleaning was achieved with purified water at room temperature, moderate fluid flow rates and without the need for chemical additives or the high power consumption associated with conventional strategies. This study illustrates the potential in harnessing an ultrasonically activated stream to remove biological contamination including brain tissue from surgical stainless steel substrates, *S. epidermidis* biofilms from glass, and fat/soft tissue matter from bone structures with considerable basic and clinical applications.

Received 24th April 2015,  
Accepted 13th July 2015

DOI: 10.1039/c5cp02406d

www.rsc.org/pccp

## 1. Introduction

The cleaning of surfaces, and in particular the removal of biological materials from an interface, is highly important in many aspects of human activity. While there are many approaches to this task, the application of ultrasonic fields<sup>1</sup> has had marked success particularly with regard to immersion of items within ‘bath’ like enclosures. However, this conventional approach has some limitations where immersion of the object to be cleaned is typically required.<sup>2</sup> This disrupts the sound field

generated in the system employed<sup>3,4</sup> and leads to the possible re-deposition of material from the essentially stagnant fluid onto uncontaminated surfaces. An alternative is the employment of a stream of fluid directed at a surface. Such an approach is described here where an ultrasonically activated stream (UAS) efficiently removes multiple biological materials from a number of different surfaces including surgical stainless steel, glass and bone. This system relies on the acoustic activation of bubbles within a fluid stream and the resultant cleaning action<sup>5</sup> at the solid/liquid interface. Note this approach is not susceptible to the typical issues associated with conventional ultrasonic cleaning. However, the fundamental mechanism, cavitation,<sup>6</sup> is extremely appealing. It is able to remove material from structured interfaces,<sup>5</sup> requires relatively low energy input,<sup>7</sup> can be deployed in a range of fluids, acts locally around the active bubbles, can generate extreme physical<sup>8</sup> and chemical<sup>9–12</sup> conditions and is an effective surface cleaning tool. Hence, if this phenomenon can be controlled<sup>13,14</sup> it has high potential for cleaning in industry, academia and the medical arena. The approach reported here harnesses this cavitation action and has a number of key features. First, the dimensions<sup>15,16</sup> and the acoustic properties<sup>17</sup> of the materials employed were chosen to provide efficient acoustic transfer through the structure and stream to a substrate. Second, a moderate fluid flow rate (33–45 cm<sup>3</sup> s<sup>-1</sup>) was employed to allow removal of material detached from the surface and maintain a continuous acoustic pathway to the substrate. Third, cleaning of the interfaces was achieved in water alone under ambient conditions (20–25 °C).

<sup>a</sup> Chemistry, University of Southampton, SO17 1BJ, UK. E-mail: prb2@soton.ac.uk

<sup>b</sup> National Centre for Advanced Tribology at Southampton, University of Southampton, SO17 1BJ, UK

<sup>c</sup> Centre for Human Development, Stem Cells and Regeneration, Medicine, University of Southampton, SO16 6YD, UK

<sup>d</sup> Centre for Biological Sciences, University of Southampton, SO17 1BJ, UK

<sup>e</sup> Institute of Sound and Vibration Research, University of Southampton, SO17 1BJ, UK

† Electronic supplementary information (ESI) available: Movie S1 Video sequence showing the generation of bubble activity in a free flowing jet as part of the UAS system reported in the main text. Note the images were recorded through a clear flat glass plate and the stream directed horizontally at the transparent interface. Hence these images were shot ‘up the stream’. Frame rate 10 kfps, shutter speed 0.1 ms. Movie S2 Video sequence showing the cleaning action of bubbles activated by sound in a free flowing jet as part of the UAS system reported in the main text. Note the images were recorded through an epoxy resin cast of a fingerprint and the stream directed horizontally at the transparent interface. The print was loaded with 0.3 μm diameter Al<sub>2</sub>O<sub>3</sub> which can be seen to be removed by the bubbles present at the solid/liquid interface. Frame rate 3 kfps, shutter speed 0.33 ms. See DOI: 10.1039/c5cp02406d

## 2. Experimental

### 2.1 The activated stream

Each UAS system consisted of a nozzle (or main section), control electronics and flow system. The UAS system was invented and developed by the University of Southampton<sup>18</sup> and has been commercialized, under licence by Ultrawave Ltd. The complete StarStream system (F0030001) can be obtained from Ultrawave Ltd. The devices used here consisted of bench-top prototypes (operating at 135 kHz) built by the University, with electronic amplifiers and signal generation using either off-the-shelf units (for example a TTI TGA12101 function generator and an E & I Type 240L power amplifier for the results of Section 3.1), or more compact electronics built by Ultrawave Ltd (for the results of Sections 3.2–3.4). During operation the liquid from the tank was gravity fed to a centrifugal pump (either Totton Pumps NDP 14/2 or Charles Austen HX8840) and then pumped through a flow meter (GEMS FT-110 Series) and into the nozzle (~10 mm diameter). In the cases of surgical instrument decontamination and biofilm removal, the nozzles also featured a copper cooling coil. For bone debridement work this was omitted. For decontamination studies the nozzles were mounted near-vertical such that liquid flowed onto the substrates from above.

High-speed images of the output flow were recorded using a Photron Fastcam APX RS camera. For the images presented the device was mounted horizontally and the flow was directed onto a piece of glass. For characterisation experiments the pressure in the stream was measured using a hydrophone (Brüel & Kjær Type 8103) and charge amplifier (Brüel & Kjær Type 2635). The hydrophone is relatively large compared with the stream diameter and so a specialised mount was constructed using a rho-c polymer. This was a block of polymer measuring 100 mm × 64 mm × 25 mm. There was a cylindrical hole (10 mm diameter and 40 mm deep) in one of the long faces (100 mm × 25 mm face), positioned such that the centre of the hole was 7 mm from the front face (100 × 64 mm face). The hydrophone was placed in the hole and surrounded with water. The block was placed under the nozzle so that the hydrophone was near to horizontal and the stream impinged on the front face of the block above the acoustic centre of the hydrophone. The distance between the nozzle exit and the top of the block was 10 mm meaning the distance between the nozzle exit and the centre of the hydrophone was  $16.8 \pm 0.3$  mm (there is an uncertainty in the exact position of the hydrophone in the hole as it is slightly smaller than the hole itself).

During decontamination studies the acoustic output of the devices was routinely monitored using a bespoke sensor system. This consisted of a piezoceramic disc sealed in rho-c polymer with an acoustic impedance matched to water. The output stream from the nozzle was directed at the surface of the disc and the voltage generated monitored as a function of time while the ultrasound was turned on. The voltage-to-pressure conversion from each sensor was quantified before use by comparison with the pressure measured using calibrated hydrophones under similar conditions. The acoustic zero-to-peak pressure

amplitudes of the UAS devices used in the decontamination studies was found to be in the range 120–250 kPa. All decontamination experiments were performed in 1 dm<sup>3</sup> purified water under aerobic conditions at 20–25 °C.

### 2.2 Decontamination of brain protein

Murine-normal brain homogenate (NBH) from C57BL mice (TSE Resource Centre, Roslin Institute, University of Edinburgh, Scotland, UK) was standardized to 1 mg ml<sup>-1</sup> in phosphate buffered saline (PBS, Gibco) with 0.1% (v/v) Tween 20 (Sigma-Aldrich). Pristine unpolished 316L surgical grade stainless steel tokens were contaminated with 1 µl (1 µg protein equivalent) drops of NBH which were allowed to dry for 24 h (~20 °C) prior to testing. Once dry the tokens were subjected to decontamination using the UAS system with two different parameters. Tokens were processed with purified H<sub>2</sub>O, at room temperature running between (33–41 cm<sup>3</sup> s<sup>-1</sup>) with no ultrasound for 5, 10, 20 and 30 s contact times. The second set of tokens were processed with purified H<sub>2</sub>O at room temperature running between (33–41 cm<sup>3</sup> s<sup>-1</sup>) with the ultrasound on for 5, 10, 20 and 30 s contact times. In both cases the stream to substrate distance was set to ~1 cm. Once processed the tokens were dried at 37 °C for 1 hour prior to staining and analysis. Total residual tissue protein on the control and processed surfaces was analysed *in situ* using the total protein blot stain, SYPRO Ruby (SR; Invitrogen, UK). The fluorescent signal was visualised using episcopic differential interference contrast (EDIC) microscopy coupled with epifluorescence (EF – Best Scientific, Wroughton, UK). Full X/Y scans of the contaminated areas were acquired at x10 objective magnification showing the SYPRO Ruby (excitation: 470 nm; emission: 618 nm) signal. The captured images were analysed using ImageJ software (National Institutes of Health) to count the total pixels of positive SR signal.

### 2.3 Decontamination of biofilms

Biofilms of *S. epidermidis* ATCC 35984, were grown on microscope glass slides in a petri plate on brain heart infusion (BHI) broth (Oxoid), at 37 °C in a humidified incubator for 72 h with media changes performed every 24 h. After the growth period the slides were removed from the petri plate, dip-rinsed twice with phosphate buffer and positioned ~1 cm from the nozzle of the UAS device. The biofilm was exposed to a water flow of 38 cm<sup>3</sup> s<sup>-1</sup> for 10 seconds with and without ultrasonic activation. Untreated biofilms (dip-rinsed) served as a negative control. Remaining biofilm was assessed qualitatively by scanning electron microscopy (SEM) and quantitatively by confocal microscopy (CM) and COMSTAT 3D image analysis of biofilm volume per unit surface area and mean biofilm thickness.

### 2.4 Debridement of trabecular bone

Human femoral heads were obtained from hematologically normal patients undergoing routine total hip replacement surgery, with approval from the Southampton Hospital Ethics Committee (LREC 194/99) and appropriate patient consent.

The femoral heads were stored at  $-80\text{ }^{\circ}\text{C}$  prior to sample preparation. A block of trabecular bone (approximately  $20\text{ mm}^3$ ) was excised from the centre of the femoral head from which  $1\text{ mm}$  thin sections were cut using a Buehler Isomet low speed precision saw. The blade of the saw was immersed in water to prevent heat-induced necrosis of the tissue sample. The slices were finally prepared as approximately  $1\text{ mm} \times 5\text{ mm} \times 5\text{ mm}$  squares using a scalpel blade and stored in phosphate buffered saline (PBS, Sigma-Aldrich Co., Ltd) overnight prior to treatment. The samples ( $n = 3$ ) were exposed for periods of 5, 10 and 20 minutes to a stream of distilled water pumped at a rate of  $33\text{ cm}^3\text{ s}^{-1}$  from a circulating reservoir. Pulsed ultrasonic activation (100 ms active, 45 ms silent) was applied in this case to the test samples and pumped water without ultrasonic activation was applied as a control along with unwashed samples. The standard clinical protocol was approximated as a further control as follows: samples were suspended in  $5\text{ cm}^3$  6%  $\text{H}_2\text{O}_2$  using a tube roller (Stuart Digital, Bibby Scientific Inc.) for 5, 10 and 20 minutes before lavage in  $2 \times 5\text{ ml}$  volumes of PBS. A further subset of samples were left in  $5\text{ cm}^3$  6%  $\text{H}_2\text{O}_2$  on a tube roller for 1 week followed by lavage in saline so as to remove virtually all soft tissue ( $>95\%$ ) and serve as a positive control for staining. Following washing, samples were fixed in 4% paraformaldehyde (Sigma Aldrich) in PBS and stored at  $4\text{ }^{\circ}\text{C}$  prior to staining. Residual connective-tissue and fat following exposure to the cleaning regimes was assessed using whole tissue histological stains. Each washed replicate from the various regimes was quartered and two samples from each replicate stained with haematoxylin (targeting cellular material) or lipid detection protocols. Weigert's haematoxylin stain was prepared using standard protocols and filtered prior to addition to samples. Samples were immersed in the stain for 10 minutes followed by a 5 minute rinse in a running water bath. The stain was differentiated by 5 rinses in acid/alcohol solution (1% HCl in 50% methanol, Sigma Aldrich) over 30 seconds and rinsed again in water before air drying. Saturated oil red O in 99% isopropanol (Sigma Aldrich) was filtered, diluted by 40% in water and filtered again before use. Samples were rinsed in 60% isopropanol for 5 minutes before immersion in oil red O working solution for 15 minutes. Samples were rinsed three times in water before immersion in PBS for imaging. Imaging was conducted using a stereomicroscope with an attached digital camera (Canon Powershot G2).

### 3. Results

#### 3.1 Removal of alumina particles from a fingerprint

The first experimental result is chosen as an example to illustrate the importance of the design of the UAS cone. The choice of design and materials, and principles of operation, for the UAS device are described at length in ref. 18. The dimensions of the stream and ultrasonic frequency were chosen to allow acoustic transfer from the cone to the free stream.<sup>15,16</sup> The cone is made of rho-c polymer and matched to the acoustic impedance of water, which allows efficient transmission of the

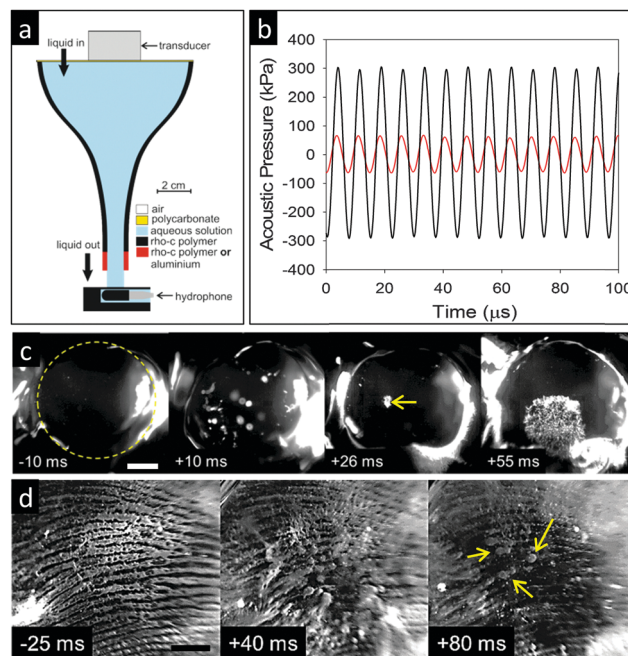


Fig. 1 (a) Materials and geometry of the ultrasonically activated stream nozzle. (b) Acoustic pressure measured in the free flowing stream in two cases: (1) using all rho-c material (—) and (2) using an aluminium end piece (—). (c) Images taken 'up the stream' (UTS) with the fluid flowing onto a sheet of glass. Scale bar 2.5 mm. The dashed circle indicates the outer edge of the flow as it impinges on the glass. (d) UTS Images of fluid flowing onto a transparent cast of a fingerprint loaded with alumina powder ( $0.3\text{ }\mu\text{m}$ ). Numerals (bottom left of each image, c and d) show the time relative to ultrasound turning on at  $t = 0$ . Scale bar 2 mm.

ultrasound from the water in the cone into the water in the stream (both the polymer and the stream being surrounded by air on the outside). If such acoustic matching is disturbed, the pressure in the stream is greatly reduced. For example if the tip of the nozzle is replaced with an aluminium section (as shown in red in Fig. 1(a)), the zero-to-peak acoustic pressure in the stream reduces from  $\sim 300\text{ kPa}$  to  $\sim 80\text{ kPa}$  (Fig. 1(b)). The effect of the higher ( $\sim 300\text{ kPa}$  zero-to-peak) acoustic pressures amplitudes on gas bubbles within the stream is shown in Fig. 1(c). Prior to ultrasonic irradiation, some gas bubbles, entrapped in the liquid as a result of the flow system, are just visible at this magnification (see Fig. 1(c),  $-10\text{ ms}$  and Movie S1, ESI†). However, after UAS activation, distinct cavitation clouds were noted (see  $+10\text{ ms}$ ). Of particular interest are clouds of bubbles generated close to the surface (see  $+26\text{ ms}$ ), which impinge on the substrate and spread laterally to cover a significant portion of the solid/liquid interface through which the images are taken ( $\sim 5\text{ mm}$  in diameter, Fig. 1(c)  $+55\text{ ms}$ ). It is these cavitation clouds which generate the cleaning action detailed in this study.

Fig. 1(d) shows just such a cleaning demonstration where a transparent impression of a fingerprint was loaded with alumina particles ( $0.3\text{ }\mu\text{m}$ ) and exposed to the fluid flow (see Fig. 1(d),  $-25\text{ ms}$ ). The alumina particles remain essentially stationary in the fluid flow until acoustically excited cavitation bubbles impinge on the surface resulting in the rapid removal

of the particles (observed streaming away from the interface, see Fig. 1(d), +40 ms and Movie S2, ESI†). After the removal of the alumina, active bubble clusters can be clearly seen on the surface of the substrate (see Fig. 1(d) +80 ms arrows). The potential of the UAS to clean a variety of biological materials, with increasing complexity, will now be examined.

### 3.2 Decontamination of brain protein

In the first example, the decontamination of surfaces pertinent to surgical instruments has been investigated. Conventional decontamination protocols for reusable surgical instruments are very efficient against microbiological contaminants. However, highly hydrophobic proteins such as prions implicated in the transmission of variant Creutzfeldt Jakob disease (vCJD) are readily adsorbed by surgical stainless steel surfaces and are difficult to remove using common decontamination protocols, resulting in a risk of potential iatrogenic infection.<sup>19–22</sup> Furthermore, the transmission of prion infectivity from surgical surfaces has been experimentally reproduced in both animal and cell bioassays.<sup>23–25</sup> Therefore, improvements in the reprocessing of surgical instruments are required to reduce the risk of iatrogenic CJD infection. For this purpose, a large number of new specialised approaches have been developed for potential use within sterile service departments (SSDs),<sup>26–30</sup> however these show (i) discrepancies in their efficacy, (ii) may be damaging to instrument surfaces or the washer disinfectors and, (iii) some advocated protocols would be too expensive or difficult to implement in current practices. In order to test the UAS technology in this arena, protein contaminated surgical surfaces were investigated. Brain tissue proteins were dried onto test 316 grade surgical stainless steel surfaces to mimic a worst case scenario where surgical instruments had been left to dry prior to decontamination. A sensitive analytical fluorescent microscopy technique<sup>31</sup> was chosen to detect the remaining contamination. Fig. 2(a and c) shows that the flow alone had a negligible effect on the removal of these proteins (~40% removed after 30 s treatment) while the activated stream system was highly efficient removing 96–99% of proteins after only a 5 second contact time (see Fig. 2(a and e)). These results are similar to those obtained with the best chemical systems currently available tested under the same conditions; however, chemical solutions require heating and have been demonstrated to still not completely eliminate prion infectivity.<sup>24,32</sup> This study unequivocally demonstrates the efficient removal of protein from surgical stainless steel surfaces using the UAS system. Although further work is required to confirm the effect of the system on prion infectivity, this study has highlighted the potential of this system as a cost-effective, rapid, facile and environmentally friendly alternative for surgical instrument decontamination.

### 3.3 Decontamination of biofilms

While the removal of proteins from surfaces is important, other more complex matrices were considered. In the next example, removal of *S. epidermidis*,<sup>33</sup> a Gram positive bacterium that is normally found on the skin of healthy individuals, was examined. This species can become pathogenic if it crosses the skin

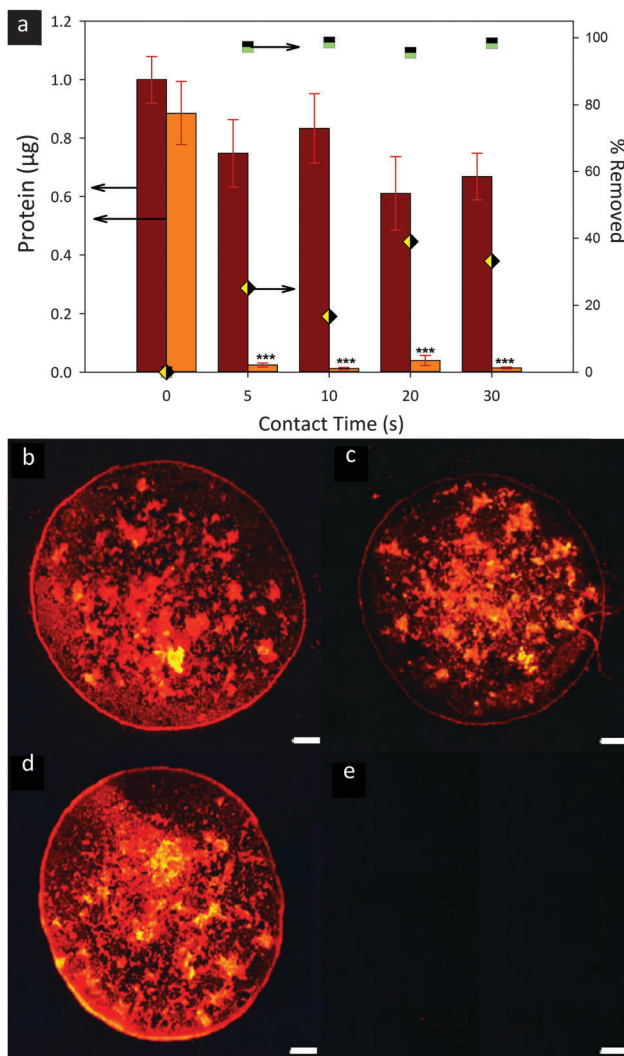
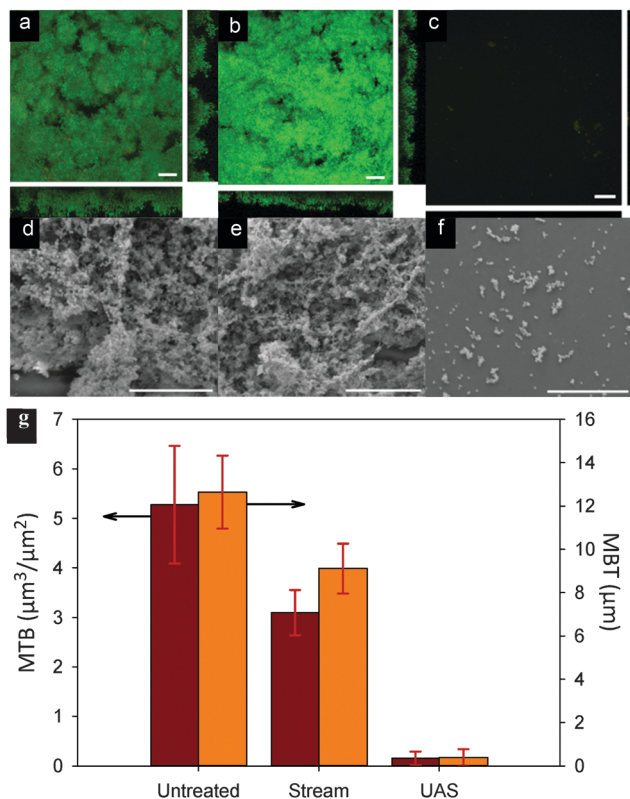


Fig. 2 (a) Assessment of protein attachment to surgical stainless steel surfaces before and after treatment with UAS. Epi-fluorescence analysis to determine the amount of residual protein and % removal as a function of time applying the water flow alone (■, ◆) or UAS (□, ◇). Error bars represent the standard error mean,  $n = 4-12$ , \*\*\* =  $P \leq 0.001$  when compared to the unwashed samples. Images (b–e) demonstrate the SYPRO Ruby stained protein on the surgical stainless steel surfaces of untreated samples (b and d), water flow alone (5 s) (c), and UAS (5 s) (e). Scale bars represent 50  $\mu\text{m}$ .

barrier through accidental or surgical wound creation. It is particularly problematic for infection of orthopaedic devices.<sup>34</sup> Fig. 3(a and d) show images of *S. epidermidis* biofilms grown for 72 hours to generate dense clusters of bacteria held together by extracellular polymeric slime (EPS). The mean biomass was  $5.3 \mu\text{m}^3 \mu\text{m}^{-2}$  of surface area with a thickness of 12.6  $\mu\text{m}$ . Exposure to the water stream alone reduced mean biofilm biomass and thickness by approximately 40 and 30% respectively (see Fig. 3g). However, this reduction was not statistically significant and a substantial amount of biofilm remained (biofilm biomass:  $P = 0.117$ ; thickness:  $P = 0.114$ ). In contrast the biofilms exposed to the activated stream were almost completely (~97% reduction in mean biomass, see Fig. 3g) removed compared to



**Fig. 3** (a–c) Images showing the confocal scanning laser microscopy (CSLM) following Syto 9 staining of *S. epidermidis* ATCC 35984 biofilms prior to treatment (control), after exposure to flow alone and after exposure to UAS respectively. (d–f) Scanning electron microscopy (SEM) images demonstrating the effectiveness of biofilm removal using UAS (f) compared to water alone (e) and the control (d). Scale bar in images (a–f) represents 25 μm. (g) Analysis of CSLM images ( $n = 6$ /treatment group) showing reduction in both mean biofilm thickness (MBT, ■) and mean total biomass (MTB, ■) compared to the water stream alone and untreated control groups. The error bars indicate the standard error in each case.

the non-treated control with relatively few clusters apparent on the substrate post treatment and a statistically significant reduction of the biomass and thickness to  $0.16 \mu\text{m}^3 \mu\text{m}^{-2}$  ( $P = 0.002$ ) and  $0.4 \mu\text{m}$  ( $P = 0.001$ ) respectively (see Fig. 3(g)).

### 3.4 Debridement of trabecular bone

Finally we have also explored the utility of the activated stream to remove soft tissue from excised bone graft. Here shortfalls in bone stock, in cases of revision arthroplasty and for void filling in various disease conditions such as avascular necrosis of the femoral head<sup>35–37</sup> are, typically, met through the use of donor bone (allograft). Allograft preparation has been shown to be of both biological and mechanical importance.<sup>38</sup> For example, residual fat and soft-tissue typically removed through dissection, hydrogen peroxide treatment and saline wash<sup>39–41</sup> results in greater necrosis within the remodelled graft<sup>41</sup> and reduction in shear strength and *in situ* stability of the initial graft preparation.<sup>40,42</sup> In order to examine the application of a UAS device for removal of fat and soft tissue in the preparation of allogeneic bone graft, freshly excised trabecular bone slices (1 mm thickness, Fig. 4) were washed using the device for up to 20 minutes.

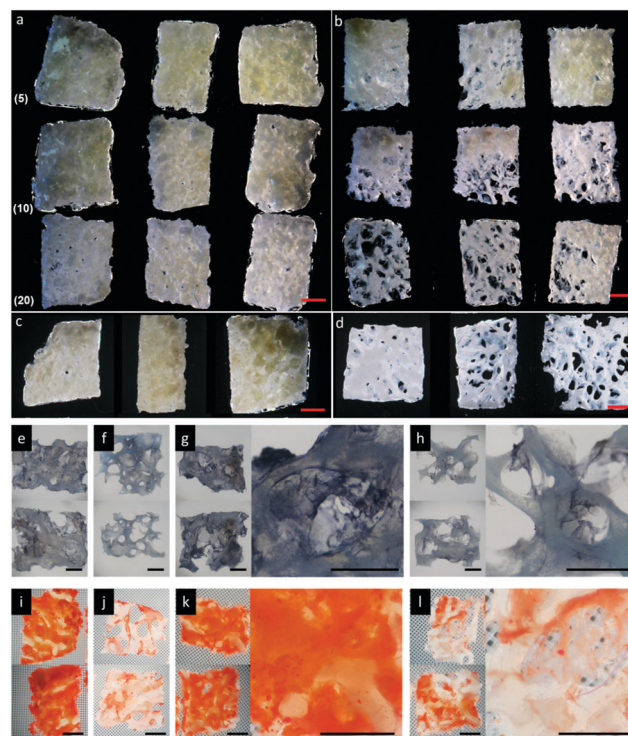


**Fig. 4** (a and b) Images showing a comparison of soft-tissue removal from freshly excised human bone material using 6%  $\text{H}_2\text{O}_2$  (a) and the UAS (b). Numbers in parenthesis show the exposure time (min) of each row of repeat samples to each treatment (relevant to both a and b). (c) Shows three examples of a negative control. (d) Shows three samples exposed to 6%  $\text{H}_2\text{O}_2$  for 1 week. The scale bars for a–d = 1 mm (—). (e–h) Shows staining for cellular material (haematoxylin). (e) represents a negative control, (f) a positive control (1 week, 6%  $\text{H}_2\text{O}_2$ ), (g) exposure to 20 minutes 6%  $\text{H}_2\text{O}_2$  and (h) exposure of a sample to 20 minutes UAS treatment. (i–l) Shows lipid (using oil red O staining). (i) Represents negative control, (j) a positive control (1 week, 6%  $\text{H}_2\text{O}_2$ ), (k) exposure to 20 minutes 6%  $\text{H}_2\text{O}_2$  and (l) exposure of a sample to 20 minutes UAS treatment. The scale bar for e–l = 0.5 mm (—).

Fig. 4(b) shows residual connective-tissue and fat following this procedure as a function of exposure time. This can be compared to preparations using standard clinical protocols (6%  $\text{H}_2\text{O}_2$  followed by lavage in saline, Fig. 4a).<sup>38,40</sup> UAS treatment removed significantly greater amounts of soft-tissue from the allograft compared with the current clinical standard and was comparable to 1 week exposure to 6%  $\text{H}_2\text{O}_2$  (Fig. 4d, f and j). Effective removal of both fat and cellularised connective tissue from within the trabecular bone matrix was confirmed through histological analysis (Fig. 4e–l). In all cases the reduction in positive staining for soft tissue after 20 minutes UAS treatment approached that observed for samples exposed to a week-long incubation in  $\text{H}_2\text{O}_2$  (see Fig. 4f and j) exemplifying the clinical potential of the UAS approach for the preparation of bone graft and the utility of UAS for the removal of tissue from micro-porous three-dimensional structures.

## 4. Conclusions

The work shown here demonstrates the versatility and diversity of the UAS approach to the decontamination of surfaces with

biological and, ultimately, clinical significance. The UAS device can create the conditions for efficient surface cleaning (e.g. appropriate acoustic pressure amplitude and a suitable bubble population) at the end of a low velocity flowing stream. These conditions were shown to remove brain proteins, biofilms and cell matrices from a variety of surfaces. The approach compares favourably with the current techniques used in the individual systems explored. In addition, this cleaning strategy avoids unnecessary chemical or thermal input to the system and operates, for the systems reported here, in water alone without the need for additives under ambient conditions.

## Acknowledgements

This work was supported by the 2011 Royal Society Brian Mercer Award (<https://royalsociety.org/grants/case-studies/tim-leighton/>) for Innovation and Ultrawave Ltd for which the authors are extremely grateful. The movies referenced in the manuscript are available as ESI.† Data supporting this study are openly available from the University of Southampton repository at <http://dx.doi.org/10.5258/SOTON/379275>.

## Notes and references

- I. E. C. Mott, D. J. Stickler, W. T. Coakley and T. R. Bott, *J. Appl. Microbiol.*, 1998, **84**, 509–514.
- T. G. Leighton, P. Birkin and D. Offin, *Proceedings of the International Congress on Acoustics*, 2013, p. 075029.
- P. R. Birkin, D. G. Offin, P. F. Joseph and T. G. Leighton, *J. Phys. Chem. B*, 2005, **109**, 16997–17005.
- C. J. B. Vian, *PhD thesis*, University of Southampton, 2007.
- D. G. Offin, P. R. Birkin and T. G. Leighton, *Phys. Chem. Chem. Phys.*, 2014, **16**, 4982–4989.
- T. G. Leighton, *The Acoustic Bubble*, Academic Press, London, 1994.
- T. G. Leighton, *Prog. Biophys. Mol. Biol.*, 2007, **93**, 3–83.
- P. R. Birkin, R. O'Connor, C. Rapple and S. S. Martinez, *J. Chem. Soc., Faraday Trans.*, 1998, **94**, 3365–3371.
- A. Weissler, *J. Am. Chem. Soc.*, 1959, **81**, 1077.
- K. S. Suslick, D. A. Hammerton and R. E. Cline, *J. Am. Chem. Soc.*, 1986, **108**, 5641–5642.
- E. B. Flint and K. S. Suslick, *Science*, 1991, **253**, 1397–1399.
- K. S. Suslick, *Sci. Am.*, 1989, **260**, 80–86.
- P. R. Birkin, D. G. Offin and T. G. Leighton, *Phys. Chem. Chem. Phys.*, 2005, **7**, 530–537.
- P. R. Birkin, J. F. Power, A. M. L. Vincotte and T. G. Leighton, *Phys. Chem. Chem. Phys.*, 2003, **5**, 4170.
- J. B. Lonzaga, D. B. Thiessen and P. L. Marston, *J. Acoust. Soc. Am.*, 2008, **124**, 151–160.
- J. B. Lonzaga, C. F. Osterhoudt, D. B. Thiessen and P. L. Marston, *J. Acoust. Soc. Am.*, 2007, **121**, 3323–3330.
- L. E. Kinsler, A. R. Frey, A. B. Coppens and J. V. Sanders, *Fundamentals of Acoustics*, John Wiley & Sons, New York, 1982.
- Cleaning apparatus and method and monitoring thereof*, WO 2011/023746, University of Southampton, 2011, International Patent application PCT/EP2010/062448 filed 26 August 2010, claiming priority from GB 0914836.2.
- H. Murdoch, D. Taylor, J. Dickinson, J. T. Walker, D. Perrett, N. D. H. Raven and J. M. Sutton, *J. Hosp. Infect.*, 2006, **63**, 432–438.
- C. J. Gibbs, D. M. Asher, A. Kobrine, H. L. Amyx, M. P. Sulima and D. C. Gajdusek, *J. Neurol., Neurosurg. Psychiatry*, 1994, **57**, 757–758.
- R. Hervé, T. J. Secker and C. W. Keevil, *J. Hosp. Infect.*, 2010, **75**, 309–313.
- I. P. Lipscomb, A. K. Sihota and C. W. Keevil, *J. Hosp. Infect.*, 2006, **64**, 193–194.
- J. A. Edgeworth, G. S. Jackson, A. R. Clarke, C. Weissmann and J. Collinge, *Proc. Natl. Acad. Sci. U. S. A.*, 2009, **106**, 3479–3483.
- J. A. Edgeworth, A. Sicilia, J. Linehan, S. Brandner, G. S. Jackson and J. Collinge, *J. Gen. Virol.*, 2011, **92**, 718–726.
- E. Flechsig, I. Hegyi, M. Enari, P. Schwarz, J. Collinge and C. Weissmann, *Mol. Med.*, 2001, **7**, 679–684.
- J. Dickinson, H. Murdoch, M. J. Dennis, G. A. Hall, R. Bott, W. D. Crabb, C. Penet, J. M. Sutton and N. D. H. Raven, *J. Hosp. Infect.*, 2009, **72**, 65–70.
- G. Fichet, K. Antloga, E. Comoy, J. P. Deslys and G. McDonnell, *J. Hosp. Infect.*, 2007, **67**, 278–286.
- K. Lemmer, M. Mielke, C. Kratzel, M. Joncic, M. Oezel, G. Pauli and M. Beekes, *J. Gen. Virol.*, 2008, **89**, 348–358.
- I. Paspaltsis, C. Berberidou, I. Poullos and T. Sklaviadis, *J. Hosp. Infect.*, 2009, **71**, 149–156.
- T. J. Secker, R. Hervé, Q. Zhao, K. B. Borisenko, E. W. Abel and C. W. Keevil, *Biofouling*, 2012, **28**, 563–569.
- R. Hervé, R. Collin, H. E. Pinchin, T. Secker and C. W. Keevil, *J. Microbiol. Methods*, 2009, **77**, 90–97.
- G. Fichet, E. Comoy, C. Dehen, L. Challier, K. Antloga, J. P. Deslys and G. McDonnell, *J. Microbiol. Methods*, 2007, **70**, 511–518.
- B. Dice, P. Stoodley, F. Buchinsky, N. Metha, G. D. Ehrlich and F. Z. Hu, *Biofouling*, 2009, **25**, 367–375.
- M. Otto, *Nat. Rev. Microbiol.*, 2009, **7**, 555–567.
- A. Aarvold, J. O. Smith, E. R. Tayton, S. Tilley, J. I. Dawson, S. A. Lanham, A. Briscoe, D. G. Dunlop and R. O. C. Oreffo, *Regener. Med.*, 2011, **6**, 461–467.
- J. Smith, A. Aarvold, E. Tayton, D. Dunlop and R. Oreffo, *Tissue Eng., Part B*, 2011, **17**, 307–320.
- A. Aarvold, J. O. Smith, E. R. Tayton, A. M. H. Jones, J. I. Dawson, S. Lanham, A. Briscoe, D. G. Dunlop and R. O. C. Oreffo, *J. Tissue Eng. Regener. Med.*, 2014, **8**, 779–786.
- I. R. McNamara, *Cell Tissue Banking*, 2010, **11**, 57–73.
- B. J. R. F. Bolland, A. M. R. New, S. P. G. Madabhushi, R. O. C. Oreffo and D. G. Dunlop, *J. Bone Jt. Surg., Br. Vol.*, 2007, **89-B**, 686–692.
- D. Dunlop, N. Brewster, S. Madabhushi, A. Usmani and C. Howie, *J. Bone Jt. Surg., Am. Vol.*, 2003, **85-A**, 639–646.
- S. van der Donk, T. Weernink, P. Buma, P. Aspenberg, T. J. J. H. Slooff and B. W. Schreurs, *Clin. Orthop. Relat. Res.*, 2003, 302–310.
- A. Bavadekar, O. Cornu, B. Godts, C. Delloye, J. Van Tomme and X. Banse, *Acta Orthop. Scand.*, 2001, **72**, 470–476.